Spring phenology and phenology-climate links inferred from two remotely sensed vegetation indices across regions and biomes

Xiyan Xu[1], William J. Riley[2], Charles D. Koven[2], Gensuo Jia[1*]

[1]Key Laboratory of Regional Climate-Environment for Temperate East Asia, Institute of Atmospheric Physics, Chinese Academy of Sciences, Beijing 100029, China

[2]Climate and Ecosystem Sciences Division, Lawrence Berkeley National Laboratory, Berkeley, California, USA

*Corresponding Author:

Dr. Gensuo Jia

Key Laboratory of Regional Climate-Environment for Temperate East Asia,

Institute of Atmospheric Physics, Chinese Academy of Sciences,

Beijing 100029, China

Email address: jiong@tea.ac.cn

Phone number: 86-10-82995314

Abstract

The timing of spring greenup (SG) as inferred by remotely sensed vegetation indices have showed contrasting dynamics across the same region and periods. Assessing the uncertainty in SG associated with different Normalized Difference Vegetation Index (NDVI) products is essential for robustly interpreting the links between climate and phenological dynamics. We compare SG inferred from two NDVI products over the period 2001-2013: (1) Terra Moderate Resolution Imaging Spectroradiometer (MODIS) and (2) National Oceanic and Atmospheric Administration's (NOAA's) Advanced Very High Resolution Radiometer (AVHRR) instruments processed by the Global Inventory Monitoring and Modeling Studies (GIMMS) to explore confidence and uncertainty in the NDVI-inferred SG trend and its links to climate variability. Both MODIS and GIMMS agreed in showing an advancement of SG in northern Canada, the eastern United States, and Russia, as well as a delay in SG in western North America, parts of Baltic Europe and East Asia. In the regions with advanced SG, GIMMS inferred much weaker advancement whereas in the regions with delayed SG, GIMMS inferred much stronger delay than MODIS. This resulted in a GIMMS SG delay in both North America and Eurasia. MODIS data show no significant SG shift in North American for spatial heterogeneity in SG shift, but dominant SG advancement in Eurasia. The SG advancement inferred from MODIS is associated with a stronger coupling between SG and temperature and a stronger sensitivity across biomes as compared to GIMMS. The main uncertainty in the SG trend and SG-temperature sensitivity are in northern high latitudes (>50°N) where GIMMS and MODIS show different magnitude and sign of the annual SG anomalies. Compared to 1988-2000, inter-biome GIMMS SG-temperature sensitivity is stable and the SG-temperature sensitivity increased in the boreal and Arctic biomes despite a slight reduction in the SG-temperature coupling over the period 2001-2013.

The explanation for the increased SG-temperature sensitivity remains unclear and requires further investigation. We suggest broader evaluation of the NDVI products against field measurements and inter-validation for robust assessment of vegetation dynamics.

Keywords: NDVI, MODIS, GIMMS, phenology, spring greenup, sensitivity

1. Introduction

Vegetation phenology plays an important role in regulating land-atmosphere energy, water, and trace-gas exchanges. As the time spanned by satellite-based Normalized Difference Vegetation Index (NDVI) products has increased to longer periods, many studies have applied NDVI products to derive spring greenup time (SG) at regional and global scales. Changes in SG have been documented in the past three decades in response to ongoing climate change (Myneni et al., 1997; Jeong et al., 2011; Zhang et al., 2013; Wang et al., 2016). The Northern Hemisphere SG has advanced in a range of 0-12 days per decade as inferred by NDVI (Table S1). The wide range of SG shifts stem from studies covering different periods and regions, and different methods and datasets that have been applied to derive phenology metrics.

Many factors associated with the obtaining of satellite data—e. g. drift of satellite orbits, calibration uncertainties, inter-satellite sensor differences, bidirectional and atmospheric effects—may cause uncertainties in satellite derived data time series and thereby the uncertainties in interpreting the vegetation dynamics. Four NDVI products have been published based on radiances collected by the Advanced Very High Resolution Radiometer (AVHRR) instruments carried by programs of NOAA/NASA Pathfinder (PAL): Global Inventory Monitoring and Modeling Studies (GIMMS), Land Long Term Data Record (LTDR) version 3 (V3) and Fourier-Adjustment, Solar zenith angle corrected, Interpolated Reconstructed (FASIR). Each of these records extends back to the year 1981. Because of their long time span, the AVHRR NDVI products have been applied in numerous regional to global vegetation phenology studies (Table 1). Advantages are recognized for GIMMS NDVI over the other AVHRR NDVI products to represent the temporal variation of NDVI (Beck et al., 2011). The more recent NDVI products retrieved from Terra Moderate Resolution

Imaging Spectroradiometer (MODIS) and Système Pour l'Observation de la Terre (SPOT) VEGETATION mission (1 km)(e.g., Durpaire et al., 1995) are considered an improvement over AVHRR for improved calibration and atmospheric corrections, and higher spatial resolution (Zhang et al., 2003).

Several inter-comparisons have been conducted to evaluate the quality of different NDVI products. Yet broad validation of NDVI products by using field measurements is limited. The SPOT-4 VGT was used to evaluate the AVHRR PAL (1998-2000) and AVHRR GIMMS (1998-2004) NDVI time series for African continent. The dynamic range of SPOT-4 VGT NDVI is generally higher than the AVHRR PAL NDVI, but matched GIMMS NDVI, implying an improvement of GIMMS over PAL (Fensholt et al., 2006), however, the growing season GIMMS NDVI is lower than MODIS NDVI in African semi-arid environment (Fensholt and Sandholt, 2005). The annual average trend of GIMMS NDVI is consistent with MODIS NDVI in the semi-arid Sahel zone, but higher discrepancies in the more humid regions (Fensholt et al., 2009). In the north 50°N, four NDVI products (GIMMS3g, GIMMSg, SeaWiFS, SPOT) except MODIS showed consistent greening trend over overlapping period although differences in growing season NDVI and magnitude of greening trend pose uncertainties in satellite vegetation dynamics (Guay et al., 2014). In mixed grassland in the Grasslands National Park of Canada, both MODIS and AVHRR NDVI cannot quantify the spatial variation in ground based leaf area index measurements (Tong and He, 2013). In Europe, SG trend inferred from GIMMS NDVI conflicted with in situ observations (Fu et al., 2015).

Despite inconsistencies and uncertainties among these NDVI products, GIMMS NDVI has been combined with other NDVI products to explore a longer period vegetation dynamics or to constrain potential data quality issue. Zhang et al.

(2013) merged GIMMS NDVI over 1982-2000 with SPOT-VGT NDVI over 2001-2011 to investigate the SG in the Tibetan Plateau. GIMMS SG over 2001-2006 was discarded for its delayed SG trend, in contrast to SPOT-VGT and MODIS SG trend, which was considered as a potential GIMMS NDVI data quality issue in the western Plateau. SG trend in Tibetan Plateau advanced by about 10.4 days decade^{-1} over 2001-2012 inferred from merged GIMMS and SPOT-VGT NDVI (Zhang et al., 2013), in contrast to the insignificant SG trend over 2000-2011 inferred from single GIMMS NDVI (Ding et al., 2016). The differences between GIMMS SG and SPOT-VGT and MODIS SG were also found after 2000s in western Arctic Russia where values and trends of MODIS and SPOT-VGT SG agreed very well (Zeng et al., 2013a). When GIMMS NDVI was stitched with MODIS NDVI, the advancing trend of spring greenup in Northern Hemisphere over 2002-2012 that was inferred from MODIS NDVI is almost 3 times larger than the trend over the period 1982-2002 inferred using the GIMMS NDVI (Wang et al., 2016). However, a similar study using the GIMMS NDVI time series over 1982-2008 revealed an insignificant advancing trend in Northern Hemisphere over 2000-2008 in relative to 1980-1999 (Jeong et al., 2011). As the different methods, when applied to the same NDVI products over the same period, can lead to consistent SG trend across regions and vegetation types (Cong et al., 2013), we hypothesize that the contradictory SG trend is due to the different NDVI products.

In this study, we attempt to (1) better understand the causes of the conflicted SG trend in previous studies, (2) analyze how much of the conflicts were contributed by the NDVI products and (3) explore how did the conflicts propagate uncertainties in understanding the vegetation dynamics and climate drivers. We compared SG as inferred by GIMMS and MODIS NDVI and their respective sensitivities to climate over the period 2000-2013, in which both the AVHRR and MODIS instruments were active. We used an independent climate reanalysis dataset to analyze the preseason, the period preceding SG during which the climate drivers regulate SG, and the sensitivity between preseason climate and SG. Data and methods are described in section 2. The results of comparison of GIMMS and MODIS SG, the preseason climate that regulates the SG and sensitivities of the SG to preseason climate are presented in section 3. Discussion and conclusions are given in section 4 and 5, respectively.

2. Data and Method

2.1 Study area and biomes

We restricted our analysis to north of 30°N, since that is the region where temperate and boreal vegetation dominates and phenology is expected to be most strongly controlled by the annual cycle of temperature (Linderholm, 2006; Fu et al. 2014; Shen et al., 2015; Güsewell et al., 2017), and regulated by water availability (Peñuelas et al., 2004; Shen et al., 2011) and photoperiod (Way and Montgomery, 2015; Singh et al., 2017) . In order to analyze the phenology and its response to climate across biomes, we used global mosaics of collection 6 MODIS data products (MCD12Q1) in the IGBP classification of land cover types with spatial resolution of 0.5° x 0.5° to mask the satellite-based SG results. The global mosaics of MCD12Q1 with geographic coordinates of latitude and longitude on the WGS 1984 coordinate reference system (EPSG: 4326) (Channan et al., 2014) were re-projected from standard MCD12Q1 with 500m resolutions (Friedl et al., 2010). We used the IGBP land cover classification for 9 biomes in 2012 (Table S1): Evergreen Needleleaf Forest (ENF), Deciduous Needleleaf Forest (DNF), Deciduous Broadleaf forest (DBF), Mixed Forest (MF), Open Shrublands (OS), Woody Savannas (WS), Grassland (GL), Permanent Wetland (PW), and Cropland (CP). We distinguish the grassland to the north of 60°N (GLN), which is more likely to be tundra, from grassland in the temperate south (GLS) due to their expected differences in climate and its controls on phenology.

2.2 Climate reanalysis

We calculated daily mean air temperature (T_m) and cumulative precipitation (P_c) from 6-hourly, half-degree resolution CRU-NCEP (Climate Research Unit-National Centers for Environmental Prediction) v6 reanalysis to identify the preseason climate associated with SG. The CRU-NCEP v6 dataset extended to 2014, is a combination of CRU TS v3.2 0.5° x 0.5° monthly climatology and NCEP reanalysis 2.5° x 2.5° with six hours time step available in near real time (http://forge.ipsl.jussieu.fr/orchidee/wiki/Documentation/Forcings).

2.3 NDVI products

We used the latest version NDVI time series (GIMMS NDVI3g) derived from the AVHRR instrument on board the NOAA satellite series. This dataset spans the period from July 1981 to December 2013 with spatial resolution of 1/12° and bimonthly temporal resolution (Pinzon and Tucker, 2014).

We also used the 16-day MODIS NDVI composites (MOD13C1, collection 6) at 0.05° spatial resolution, and further performed data quality control. We regridded both GIMMS and MODIS NDVI data to 0.5° x 0.5° resolution by taking the mean value in a 0.5° x 0.5° pixel to match the spatial resolution of the CRU-NCEP reanalysis. We screened the pixels with annual maximum NDVI <0 to exclude the non-vegetated pixels. For GIMMS NDVI3g, the algorithm has improved snow-melt detection and the pixels recognized with snow or ice were filled with average seasonal profile or spline interpolation (Pinzon and Tucker, 2014). The pixels flagged with snow/ice were given the NDVI values with the values from the previous nearest period without snow influence. Even though, the filled values are very close to zero in the dormant season and the near-zero values are smoothed by the double logistic method or piecewise logistic method described in section 2.3. SGs were derived from GIMMS NDVI 2001-2013 to fit the time period of MOD13C1 NDVI product.

2.4 Determination of SG and preseason climate

We determined the preseason duration following the method of Shen et al. (2014), but with a different climate reanalysis product and a different method for calculating SG. The common used regression methods to reconstruct NDVI time series and derive SG include Savitzky-Golay fitting method, spline smoothing, asymmetric Gaussian functions, double logistic function, and harmonic analysis of times series. These methods are valid in fitting NDVI gaps and reducing noise (Cai et al. 2017), however, can make differences in estimating phonological stages (Cong et al., 2013). In order to reduce the mixed uncertainty of reconstruction methods and NDVI products, here we used one regression method to reconstruct the NDVI series. The double logistic method uses least-square fitting to half growing season (Zhang et al., 2003). It is more robust than other methods in reducing noise (Hird and McDermid, 2009) and estimating the vegetation seasonal dynamics, when there is no local calibration (Cai et al., 2013). As we applied the double logistic method to a single growth cycle, it is reliable to smooth noise (Atkinson et al., 2012).

Day of SG and mean day of SG

We first applied double logistic method (Zhang et al., 2003) to fit and smooth the temporal variation of NDVI to vegetation growth：

$$y(t) = \frac{c}{1+e^{a+bt}} + d \quad (1)$$

where t is time in days, $y(t)$ is the vegetation index at time t, a and b are fitting parameters, $c+d$ is the maximum vegetation index value, and d is the initial background vegetation index, usually the minimum vegetation index value preceding the growing season. D_{SG} is identified as the Julian date at which the rate of change in the vegetation growth ($y(t)$) is maximum. D_{SG} is the maximum of the curvature and derived as the second derivative of equation (1) . The mean D_{SG} ($\overline{D}_{SG}$) in each pixel is averaged over the analysis years. For the pixels with multiple growth cycles in a year, we applied this double logistic method to the first cycle, so that D_{SG} is the Julian date at which the second derivative of $y(t)$ is maximum for the first time in a year.

Preseason period and preseason climate

We calculated the preseason period separately for temperature and precipitation. To do this, we first calculated T_m and P_c during the respective preseason periods. We defined the preseason climate (T_m and P_c) in each pixel over the period preceding $\overline{D}_{SG}$ from 15 to 120 days with an increment of 3 days. We expect the relative variation in precipitation to be more relevant than absolute values in determining phenology, thus we used the relative variation of cumulative precipitation in percentage (%) of precipitation change instead of the absolute cumulative precipitation variation in millimeter (mm). We detrended the calculated T_m and P_c over the historical period. For each period preceding $\overline{D}_{SG}$ for a given pixel, we calculated the Pearson's correlation coefficients (PCC) between D_{SG} and T_m (and P_c). We screened the data to remove pixels where we found a positive interannual correlation between (1) preseason temperature and D_{SG} and (2) preseason precipitation and D_{SG}, respectively. We defined the period with the most negative correlation between D_{SG} and T_m (and P_c) as the preseason P_T (and P_P). The length of preseason (days) for temperature and precipitation control is defined as L_{PT} and L_{PP}, respectively. The superscript of G and M represents the variables derived from GIMMS and MODIS, respectively (e.g. D_{SG}^{M} and L_{PT}^{M} are D_{SG} *and* L_{PT} derived from MODIS, respectively.).

SG response to preseason climate

We calculated the response of SG to preseason climate by calculating linear regressions between D_{SG} and T_m (and P_c). We excluded the SG response to preseason climate in pixels where no significant relationship was found (i.e., p-value > 0.1).

3. Results

3.1 MODIS and GIMMS SG comparison

The spatial pattern of GIMMS-inferred mean D_{SG} ($\overline{D}_{SG}^{G}$) and MODIS-inferred D_{SG} ($\overline{D}_{SG}^{M}$) is consistent (r = 0.83, p < 0.01). The regions with evident difference between D_{SG}^{G} and D_{SG}^{M} are in the circumpolar Arctic and Asia high-altitudes where correlations between the time series of D_{SG}^{G} and D_{SG}^{M} are relatively low (Figure 1a and b). About 47% of the pixels in the north of 30°N have the inter-annual correlation above 0.5 (p < 0.1), 86% of which are located between 45-90°N. The better correlated D_{SG}^{G} and D_{SG}^{M} time series to the north of 45°N than in lower latitudes implies agreed inter-annual variation of D_{SG}^{G} and D_{SG}^{M} in this region. In the regions with well-correlated inter-annual variation, D_{SG} differences between MODIS and GIMMS still show significant latitudinal characteristics (Figure 1b). In the northern mid-latitudes, we inferred a later $\overline{D}_{SG}$ using MODIS (9±16days) in 67% of the pixels, and an earlier $\overline{D}_{SG}$ (5 ± 4 days) in the remaining pixels, as compared to GIMMS. We also inferred a later $\overline{D}_{SG}$ using MODIS in southern Asia and the eastern United States as compared to $\overline{D}_{SG}$ using GIMMS (Figure S1). The D_{SG}^{G} and D_{SG}^{M} inter-annual variation are weakly correlated in the southern mid-latitudes, especially in the Eurasia. For those pixels in the south of mid-latitude, where inter-annual variation of D_{SG}^{G} and D_{SG}^{M} are well correlated, D_{SG}^{M} advanced D_{SG}^{G} by 6±5 days (Figure 1b).

Both MODIS and GIMMS agreed in showing that D_{SG} advanced in Northern Canada, Eastern United States, and Russia, and that D_{SG} delayed in western North America, parts of Baltic Europe and East Asia (Figure 1c and 1d). In the regions where D_{SG} advanced, D_{SG}^{G} advancement was much weaker than D_{SG}^{M}. In the regions where D_{SG} delayed, the D_{SG}^{G} delay is much stronger than D_{SG}^{M}. Together, these differences lead to a delayed continental-scale D_{SG}^{G} trend in both North America (0.85 days yr^{-1}) and Eurasia (0.33 days yr^{-1}) at 95% confidence level. MODIS implied a slight delay of 0.18 days yr^{-1}in North American but a significant advanced SG trend of 1.00 days yr^{-1} in Eurasia at 90% confidence level. The differences in D_{SG}^{G} and D_{SG}^{M} trend are mainly in the northwest of North America and east-to-central Eurasia north of 50°N. The inter-annual variability of D_{SG} anomalies in relative to $\overline{D}_{SG}$ over 2001-2013 indicated consistent anomaly signs of D_{SG} between MODIS and GIMMS over 30-50°N (Figure 2a, c and e). The most remarkable difference in D_{SG} anomaly between MODIS and GIMMS is in the north of 50°N (Figure 2b). It is mainly due to negative D_{SG}^{G} anomalies over 2001-2008 and positive D_{SG}^{G} anomalies thereafter in North America, in opposite to D_{SG}^{M} anomalies (Figure 2d). In Eurasia, both MODIS and GIMMS indicated anomalies of advanced D_{SG} in the north of 50°N after 2006 (Figure 2f). A large transition in the D_{SG}^{G} anomaly occurred around 2000. The transition is particularly remarkable in North America, which is due to a 5-6 days later mean D_{SG} ($\overline{D}_{SG}^{G}$) over 2001-2013 than that over 1982-2000 in North America.

3.2 Preseason climate regulating SG

The preseason length of temperature control for GIMMS (L_{PT}^{G}) and MODIS (L_{PT}^{M}) that we inferred from the correlation between T_m and D_{SG} differed due to the differences between D_{SG}^{G} and D_{SG}^{M}(Figure S2a and S2b). The spatial pattern of L_{PT}^{G} shows significant heterogeneity, with L_{PT}^{G} over two months in the regions from Russia to central Asia in Eurasia and from Alaska to northwestern Canada in North America. L_{PT}^{G} is 62±38 days for all the valid pixels, while L_{PT}^{M} is usually less than two months, with the L_{PT}^{M} of 41±31days. Moreover, L_{PT}^{M} is better correlated to T_m during its corresponding preseason (P_T^M) with North Hemisphere correlation of 0.6±0.2 in comparison to the correlation between D_{SG}^{G} and T_m during its preseason (P_T^G) of 0.3±0.2 (Figure 3a and 3b).

The fraction of the northern mid- to high-latitude land surface correlated with preseason precipitation is less than that correlated with temperature for both GIMMS and MODIS (Figure 3 and Figure S2). The preseason length of precipitation control for MODIS (L_{PP}^{M}= 56±35 days) is longer than that of temperature control. In contrast, GIMMS showed relatively shorter preseason length of precipitation control (L_{PP}^{G} = 45±32 days) than that of temperature control. Although GIMMS showed a larger fraction of land surface where precipitation correlated to D_{SG} than MODIS, MODIS and GIMMS showed consistent spatial pattern in both preseason length and correlations between P_c and D_{SG}(Figure 3c and 3d). The mean PCC is -0.4±0.2 for both MODIS and GIMMS.

The spatial pattern of the temperature trend in P_T^M and P_T^G over 2001-2013 is consistent (r = 0.61, p < 0.01) although the derived preseason length for temperature control differed for GIMMS and MODIS derived D_{SG} (Figure S3a and S3b). The majority of both North America and North Eurasia experienced warming of the SG preseason, while Alaska, the eastern edge of Hudson Bay and the mid-latitudes of Eurasia (40-60°N) experienced a preseason cooling. The preseason warming trend is most significant in central Russia and eastern Canada and the cooling trend is most significant in part of Central Asia and central to eastern China. The maximum preseason warming trend is about 0.6 °C yr^{-1} in central Russia. The precipitation trend in the preseason is insignificant and more heterogeneous as compared to the temperature trend for both P_P^M and P_P^G (Figure S3c and S3d). The spatial pattern of the precipitation trend in P_P^M and P_P^G are also less correlated ($r = 0.40$, $p < 0.01$) than that of temperature trend. Wetting of the preseason occurred in mid to east of the United States, Western Canada, Northern Norway and Northwestern Russia. The largest value of the wetting trend is about 7 mm yr^{-1}. Drying preseason only occurred remarkably in the southeastern the United States and scattered in Eurasia. The pixels where the largest values of a preseason drying trend is about 4 mm yr^{-1}.

3.3 SG sensitivity to preseason climate

The fraction of areas in which D_{SG}^M sensitive to T_m and P_c are much larger than D_{SG}^G (Table S2) and D_{SG}^M are more sensitive to T_m and P_c in relative to D_{SG}^G (Figure 4). About 43% of the land fraction shows significant sensitivity of D_{SG}^M to T_m ($p < 0.1$) compared with 13% of the land fraction with significant sensitivity of D_{SG}^G to T_m. About 11% of the land fraction shows significant sensitivity of D_{SG}^M to P_c ($p < 0.1$) as compared with 3% of the land fraction with significant sensitivity of D_{SG}^G to P_c. The sensitivity of D_{SG}^M to T_m is most significant in the mid- to high-latitudes (Figure 4b) whereas the sensitivity of D_{SG}^M to P_c is scattered (Figure 4d). The mean sensitivity of D_{SG}^M to temperature is about -3.58 days per °C warming in preseason, which almost doubles the mean sensitivity of D_{SG}^G to temperature of -1.70 days $°C^{-1}$. The mean sensitivity of D_{SG}^{G} to precipitation is about -0.16 days advancement per percent of precipitation increase in relative to the mean P_c over 2001-2013, which is close to the mean sensitivity of D_{SG}^{M} to precipitation of about -0.13 days $\%^{-1}$. Due to the weak SG-precipitation coupling and sensitivity, we only analyzed biome-scale sensitivity of D_{SG} to T_m sensitivity (Figure 5). The difference between the sensitivity of D_{SG} to T_m as inferred by MODIS versus GIMMS is less in forest biomes, even though D_{SG}^{M} is more sensitive to T_m in all the biomes in relative to D_{SG}^{G}. The differences in D_{SG} to T_m sensitivity are especially significant in northern biomes. For example, sensitivity of D_{SG}^{M} to T_m in open shrublands, northern grasslands, and permanent wetlands are 50% higher than sensitivity of D_{SG}^{G} to T_m in these biomes.

As the GIMMS NDVI product extends as far back as the early 1980s, we also performed the comparison of D_{SG}^{G} to T_m sensitivity over two periods. D_{SG}^{G} to T_m sensitivity was analyzed with the same method in section 2, but between the period spanning 1988 and 2000. This has the same length of time (13 years) as the later analysis period of 2001-2013. The fraction of area where D_{SG}^{G} shift in response to T_m and P_c is reduced in the period 2001-2013 as compared to the earlier 1988-2000 (Table S2). Most of the biomes show a slightly increased sensitivity of D_{SG}^{G} to T_m in the later period, as compared to that over 1988-2000, with the highest increase in the northern grasslands (44.6%) and open shrublands (41.2%) (Figure 5a). The sensitivity of D_{SG}^{G} to T_m is relatively stable in southern grasslands. Exceptionally, the sensitivity of D_{SG}^{G} to T_m declined by 1.4 days °C^{-1} for deciduous broadleaf forests and 0.1 days °C^{-1} for mixed forests; this represents a reduced sensitivity of 33.7% and 3.4% respectively. The inter-biome variation of the sensitivity of D_{SG}^{G} to T_m is stable (r = 0.90, $p < 0.001$) over the two periods (Figure 5b).

4. Discussion

4.1 SG mean state and trend

We analyzed MODIS and GIMMS NDVI products to infer spring greenup dates and their responses to preseason climate over the period 2001-2013. Inter-annual variation of greenup date as inferred from MODIS and GIMMS are well correlated north of 45ºN (86% of the pixels with $r > 0.5$ and $p < 0.1$). But in these regions, we tend to infer a later greenup time using MODIS than GIMMS NDVI. This may be contributed by the evergreen vegetation (Gamon et al., 2016) and the influences of snow cover on the boreal pixels (Moulin et al., 1997). The foliage amount of evergreen vegetation has little change through seasons, therefore the photosynthetic phenology is difficult to detect by satellite remote sensing (Gamon et al., 2016). The snow cover affects the greenup determination in two ways. On the one hand, the snow cover led to NDVI gaps during the dormancy season. As a result, the time series of NDVI cannot be adequately fitted during the transitional snow melting and vegetation greening season (Zhou et al., 2015). We filled the snow-flagged MODIS NDVI with NDVI from previous period without snow contamination, whereas GIMMS NDVI was filled with average seasonal profile or spline interpolation (Pinzon and Tucker, 2014). Our MODIS filling potentially underestimate the NDVI during the transition season. On the other hand, the overlapped time of snowmelt and greenup leads complexity in greenup determination. In high latitudes with seasonal snowpack, the beginning of the growing season is often determined by snowmelt rather than temperature (Semenchuk et al., 2016). The study over Yamal Peninsula revealed that spring greenup date is almost the same as snow-end date between 70.0-73.5ºN (Zeng and Jia, 2013), so that the snow cover affects the accuracy in identifying vegetation greenup. In the northern high latitudes at the selected locations in Canada and Sweden, even if the pixels influenced from snow cover are excluded, MODIS NDVI is lower than GIMMS NDVI in the dormant season (Fensholt and Proud, 2012). This can make an explanation to the late transition from dormant season to growing season by MODIS.

We inferred a heterogeneous trend in SG using both MODIS and GIMMS, but the sign and magnitude of the SG shift varies between MODIS and GIMMS. The main difference between the trend in SG as inferred by MODIS and GIMMS is in Alaska and Siberia, which lead to the main uncertainties in the NDVI derived SG trend in the northern high latitudes. The significant GIMMS SG delay in Alaska and mid-latitude Eurasia lead to a general delay in SG in North America and Eurasia. In contrast, we inferred a delay in SG using MODIS in southern Alaska and eastern Canada offset SG advancement in eastern the United States and Canada, resulting in insignificant SG trend in North America. Significant SG advancement in Siberia resulted in strong SG advance in Eurasia. Even so, MODIS and GIMMS showed large inter-annual variability of SG anomalies in relative to the mean SG over 2001-2013 and the signs of the anomalies are consistent in between 30ºN and 50ºN. MODIS NDVI inferred mean SG advancement of 0.96 days year^{-1} between 52-75ºN over 2001-2013 at 90% confidence level in our results, which overwhelmed the MODIS snow-end date advancement of 0.37 days year^{-1} in this region over 2001-2014 (Chen et al., 2015). The lagged snow phenology advancement implies that snow complication in determine SG in the cold regions is still present at a warmer climate. To reduce the snow effect on spring phenology determination, the normalized difference water index method (Delbart et al., 2004; Delbart et al., 2006), plant phenology index method (Jin et al. 2017), normalized difference vegetation index- normalized difference infrared index phase-space method (Thompson et al., 2015) are alternatives to improve the NDVI-based phonological metrics.

4.2 SG dates sensitivities to climate

The SG to preseason climate sensitivity by MODIS and GIMMS showed varied degree of vegetation-climate seasonal coupling. The differences in MODIS and GIMMS SG propagate the conflicts to the preseason length. However, the L_{PT}^{M} is very close to L_{PT}^{G} (=43±30days) in an earlier longer period over 1982-2005 (Xu et al., 2018). The higher correlation between MODIS SG and preseason temperature indicates stronger MODIS SG-climate relationships. The consistent preseason length inferred from MODIS over 2001-2013 and GIMMS over 1982-2005, and stronger MODIS SG-temperature coupling indicate more reliable MODIS NDVI in the available period and GIMMS NDVI data in the earlier period. The stronger MODIS NDVI to temperature correlation than GIMMS NDVI was also reported in central Europe, where the correlation between temperature and August NDVI anomalies were analyzed (Kern et al., 2016). The stronger SG-temperature coupling than precipitation is consistent with our previous study of SG to climate sensitivity over 1982-2005 (Xu et al., 2018). MODIS inferred stronger SG-temperature sensitivity in the northern boreal and Arctic biomes can be explained by the site-level observation that temperature sensitivity of phenology is greater in colder, higher latitude sites than in warmer regions (Prevéy et al., 2017). At the colder sites, the small changes in temperature may constitute greater relative changes in thermal budget (Oberbauer et al., 2013), so that the warming impacts on vegetation are amplified. This explanation is not applicable to the GIMMS NDVI inferred SG response to temperature that vegetation with earlier growing season is more sensitive to temperature (Shen et al., 2014).

The sensitivity of GIMMS SG to temperature increased over 2001-2013 in relative to that over 1988-2000. Our results showed SG to temperature sensitivity increased most significantly in Arctic grassland (44.6%), followed by other boreal biomes (open shrubland (41.2%), permanent wetland (35.9%), woody savanna (31.1%) and deciduous needleleaf forest (17.6%)). The magnitudes of enhanced sensitivity are even larger when we compare 2001-2013 SG-temperature sensitivity with a longer period over 1982-2005 (Xu et al., 2018). Compare with the period 1982-2005, SG-temperature sensitivity of the northern biomes (deciduous needleleaf forest, woody savanna, open shrublands and permanent wetlands) all increased more than 50% over 2001-2013 with stable inter-biome sensitivity variation ($r = 0.91$, $p < 0.01$).

The increased sensitivity of SG to temperature for boreal biomes has not been well investigated. In the contrary, temperature sensitivity of spring greenup may decline under warmer climate because (1) insufficient winter chilling may delay the spring greenup in spite of continued spring warming (Yu et al., 2010), (2) when spring greenup starts earlier, shorter photoperiod can limit the potential of leaf development (Chmielewski & Götz, 2016), (3) greenup may respond nonlinearly to temperature and be saturated at a high temperature (Caffarra & Donnelly, 2011), and (4) under warmer condition, the preseason duration of thermal forcing can be reduced, which declines the SG-temperature sensitivity (Güsewell et al., 2017). The vegetation growth (represented by NDVI) to temperature sensitivity was reported declining in the growing season (April-October) based on GIMMS NDVI over 1982-2012 linked to water stress (Piao et al., 2014). In temperate ecosystems, the lower NDVI to temperature sensitivity coincidently occurred with increased drought events. While in the arctic ecosystem, the lowered sensitivity of NDVI to temperature may be explained by increases in heat waves because the physiological response of photosynthesis to temperature is nonlinear with lower sensitivity under warmer conditions (Piao et al., 2014). The higher interannual temperature variability can also cause higher variations in water supply, thus the declined coupling between vegetation growth and interannual variability of growing season temperature, generally in semiarid regions (Wu et al., 2017). The wetting preseason in mid to east of the United States, Western Canada, Northern land along Norway and Northwestern Russia may partly enhanced SG-temperature if the enhancement is validated.

4.3 Uncertainties in SG as derived by MODIS and GIMMS NDVI

With SG as inferred using GIMMS over the period 1988-2000 and as inferred using MODIS over 2001-2013, we found that the trend is advanced continuously in response to a continuing trend in preseason warming. The uncertainties in the SG trend and its climatic sensitivity arise when SG as inferred using GIMMS, MODIS, and other sensors and in situ observations are compared together over a similar period after 2000, during which the main conflicts in SG trend were found. Our results coincide with other studies that GIMMS NDVI inferred an opposite trend of SG before and after 2000 in the circumpolar Arctic (Park et al., 2016). SPOT VGT retrieved a continuously advanced SG trend over 1999-2013 in the circumpolar region (>45 °N), in consistent with MODIS SG, although the magnitude and spatial distribution of the advancement are different between SPOT and MODIS (Gonsamo and Chen, 2016). Wang et al. (2016) and Zhang et al. (2013) proposed that quality issues may present in GIMMS NDVI, which can bias vegetation growth sensitivity and growth trend. Instead of using continuous GIMMS SG over 1982-2011, Zhang et al. (2013) merged datasets of GIMMS SG over 1982-2000 and SPOT-VGT SG over 2001-2011 to detect SG trend due to data quality issues with GIMMS NDVI in most parts of western Tibetan Plateau, according to the findings of opposite GIMMS SG trend to SPOT-VGT and MODIS SG trend over the period 2001-2006. With this merged data record, the SG trend continuously advanced in Tibetan Plateau over

1982-2011. This result is consistent with the SG trend derived from tree-ring data (Yang et al., 2017). On the contrary, continuous GIMMS SG over 1982-2006 inferred delayed SG trend after mid-1990s over Tibetan Plateau (Yu et al., 2010). At the North Hemisphere scale, GIMMS SG (1982-2008) showed significant decadal variation and declining SG shift: advanced 5.2 days over 1982-1999, but only advanced 0.2 days over 2000-2008 (Jeong et al., 2011). However, the merged GIMMS (1982-2006) and MODIS (2002-2012) showed SG shift over 2002-2012 (-6 days decade^{-1}) is about three times larger than that over 1982-2002 (-2 days decade^{-1}), which is interpreted as enhanced SG advancement and its response to temperature over time (Wang et al., 2016). For the varied timing of SG derived from different products, Zhang et al. (2017) suggested intersensor calibrations to reduce the difference between vegetation index products and exclusion of the low quality phenology timing. The ground observations are solutions to validate the remote sensed phenology. However, in situ observations and remote sensed phenology differed no matter how accurate they are retrieved (Gonsamo and Chen, 2016), due to the scale and resolution issues.

These SG shift uncertainties after 2000 are more likely to be explained by the differences in the NDVI products that implied the opposite SG trend, anomalies north of 50ºN and biome-scale SG-temperature sensitivities. The spectrum range difference of MODIS and AVHRR sensor channels is a main contribute to the NDVI differences. MODIS NDVI is derived from bands 1(620-670nm) and 2 (841-876nm) of the MODIS on board NASA's Terra satellite whereas GIMMS NDVI is derived from bands 1(580-680nm) and 2 (725-1100nm) of AVHRR. Furthermore, the NDVI by MODIS and GIMMS were retrieved from a different spatial resolution. The retrieved NDVI is a mixture of different vegetation species with diverse phenologies, bare soil and even water bodies dependent on the spatial resolution (Helman, 2018). Both

GIMMS NDVI3g and MOD13C1 were generated using daily surface reflectance product to a similar composite interval. However, the MODIS applied the constrained-view angle-maximum value composite while GIMMS applied maximum value composite. The maximum value composite cannot completely remove atmospheric effect (Pinzo and Tucker 2014) and the different composite technique can cause the value difference in the same interval (Gallo et al., 2004).

The large GIMMS SG anomaly transition around 2000 may be associated with the sensor transition from AVHRR/2 to AVHRR/3, although among-instrument AVHRR calibration were conducted with NDVI data derived from Sea-Viewing Wide Field-of-view Sensor (SeaWiFS) (Pinzon et al., 2014). The calibration with SeaWiFS is considered as an improvement of GIMMS NDVI in the very northern latitudes (Marshall et al, 2016). Even so, the data issues associated with sensor transition, such as (1) satellite signal degradation through lifetime, (2) band design, (3) effect of maximum value composite (MVC) and (4) replacement of satellites in NOAA series, potentially influence the interpretation of the SG trend and its sensitivity to climate drivers.

5. Conclusions

We compare the MODIS and GIMMS NDVI inferred time of spring greenup and its response to preseason climate over 2001-2013. We infer a spring greenup delay using GIMMS NDVI in both North America (0.80 days yr^{-1}) and Eurasia (0.22 days yr^{-1}), whereas, using MODIS NDVI, we infer no significant spring greenup shift in North American and an advanced SG trend of 0.78 days yr^{-1} in Eurasia. The differences in MODIS and GIMMS inferred spring greenup trend are mainly in northern high latitude (>50ºN). The differences are implied by opposite anomalies in the time of spring greenup in North America and a large GIMMS inferred spring greenup transition around 2000 that maybe explained by data issues associated with the sensor transition from AVHRR/2 to AVHRR/3, including (1) satellite signal degradation through lifetime, (2) band design, (3) effect of maximum value composite (MVC) and (4) replacement of satellites in NOAA series. Temperature is the primary climate driver of the time of spring greenup for both MODIS and GIMMS, although MODIS inferred both a stronger sensitivity and correlation between SG and temperature. The opposing trends of SG as inferred using MODIS and GIMMS resulted in differing SG to temperature sensitivity across biomes (-3.6±0.7 days °C^{-1} for MODIS and 2.2 ± 0.8 days °C^{-1} for GIMMS). Using GIMMS, we inferred that the sensitivity of greenup to temperature, which increases over time for Arctic and boreal biomes, cannot be well explained by the mechanisms regulating the sensitivity of SG under a warming climate. This result requires further investigation. Our results suggest the importance of snow-vegetation interactions in high latitude vegetation monitoring and inter-validation of multiple datasets to better assess vegetation dynamics.

Acknowledgements

This study is funded by the Strategic Priority Research Program of the Chinese Academy of Sciences, CASEarth (XDA19070203), grants from Natural Science Foundation of China (NSFC #41590853 and #41875107) and CAS Pioneer Hundred Talents Program. We acknowledge support from the U.S. Department of Energy, Office of Science, Biological and Environmental Research, Regional and Global Climate Modeling Program through the RUBISCO Scientific Focus Area under contract DE-AC02-05CH11231 to Lawrence Berkeley National Laboratory.

The authors declare no conflicts of interest.

Supplements

Figure S1

Figure S2

Figure S3

Table S1

Table S2

Reference

Atkinson, P. M., C. Jeganathan, J. Dash, C. Atzberger (2012). Inter-comparison of four models to smoothing satellite sensor time-series data to estimate vegetation phenology. Remote Sensing of Environment, 123, 400-417.

Beck, H. E., T. R. McVicar, A. I. J. M. van Dijk, J. Schellekens, P. A. M. de Jeu, L. A. Bruijnzeel (2011). Global evaluation of four AVHRR-NDVI data sets: intercomparison and assessment against Landsat imagery. Remote Sensing of Environment, 115, 2547-2563.

Brown, M. E., J. E. Pinzón, K. Didan, J. T. Morisette, C. J. Tucker (2006). Evaluation of the consistency of long-term NDVI time series derived from AVHRR, SPT-Vegetation, SeaWiFS, MODIS, and LandSAT ETM+Sensors. IEEE Transactions on Geosciences and Remote Sensing, 44, 1787-1793. DOI:1O.1109/TGRS.2005.860205

Caffarra, A., A. Donnelly, I. Chuine, M. B. Jones (2011). Modelling the timing of Betula pubescens budburst. I. Temperature an photoperiod: A conceptual model. Climate Research, 46, 147-157.

Cai, Z., P. Jönsson, H. Jin, L. Eklundh (2017). Performance of smoothing method for reconstructing NDVItime-series and estimating vegetation phenology from MODIS data. Remote Sensing, 9, 1271, doi:10.3390/rs9121271.

Channan, S., K. Collins, and W. R. Emanuel (2014). Global mosaics of the standard MODIS land cover type data. University of Maryland and the Pacific Northwest National Laboratory, College Park, Maryland, USA.

Chen, X., S. Liang, Y. Cao, T. He, D. Wang (2015). Observed contrast changes in snow cover phenology in northern middle and high latitudes from 2001-2014. Scientific Report, 5, 16820, DOI: 10.1038/srep16820.

Chmielewski, F. M., & Götz, K.-P. (2016). Performance of models for the beginning of sweet cherry blossom under current and changed climate conditions. Agricultural and Forest Meteorology, 218–219, 85–91.

Cong, N., T. Wang, H. Nan, Y. Ma, X. Wang, R. B. Myneni, S. Piao (2013). Changes in satellite-derived spring vegetation green-up date and its linkage to climate in China from 1982 to 2010: a multi-method analysis. Global Change Biology, 19, 881-891, doi:10.1111/gcb.12077.

Delbart, N., L. Kergoat, T. Le Toan, J. Lhermitte, G. Picard (2005). Determination of phenological dates in boreal regions using normalized difference water index. Remote Sensing of Environment, 97, 26–38.

Delbart, N.,T. Le Toan, L. Kergoat, V. Fedotova (2006). Remote sensing of spring phenology in boreal regions: A free of snow-effect method using NOAA-AVHRR and SPOT-VGT data (1982-2004). Remote Sensing of Environment, 101, 52–62.

Durpaire, J. P., T. Gentet, T. Phulpin, and M. Arnaud (1995). "Spot-4 Vegetation Instrument: Vegetation Monitoring on a Global Scale." Acta Astronautica, 35, 453-459.

Fensholt, R. and I. Sandholt (2005). Evaluation of the MODIS and NOAA AVHRR vegetation indices with in situ measurements in a semi-arid environment. International Journal of Remote Sensing, 26, 2561-2594.

Fensholt, R., T.T. Nielsen, S. Stisen (2006). Evaluation of AVHRR PAL and GIMMS 10-day composite NDVI time series products using SPOT-4 vegetation data for the African continent. International Journal of Remote Sensing, 27, 13, 2719-2733, DOI:10.1080/01431160600567761

Fensholt, R., K. Rasmussen, T. T. Nielsen, C. Mbow (2009). Evaluation of earth observation based long term vegetation trends-intercomparing NDVI time series trend analysis consistency of Sahel from AVHRR GIMMS, Terra MODIS and SPOT VGT data. Remote Sensing of Environment, 113, 1886-1898.

Fensholt, R. and S. R. Proud (2012). Evaluation of Earth Observation based global long term vegetation trends- Comparing GIMMS and MODIS global NDVI time series. Remoste Sensing of Environment, 119, 131-147.

Friedl, M.A., D. Sulla-Menashe, B. Tan, A. Schneider, N. Ramankutty, A. Sibley and X. Huang (2010). MODIS Collection 5 global land cover: Algorithm refinements and characterization of new datasets, 2001-2012, Collection 5.1 IGBP Land Cover, Boston University, Boston, MA, USA.

Fu, Y. H., M. Campioli, Y. Vitasse, H. J. De Boeck, J. Van den Berge, H. AbdElgawad, H. Asard, S. Piao, G. Deckmyn, I. A. Janssens (2014). Variation in leaf flushing date influences autumnal senescence and next year's flushing date in two temperate tree species. Proceedings of the National Academy of Sciences of the United States of America, 111, 7355-7360. https://doi.org/10.1073/pnas.1321727111

Fu, Y. H., S. Piao, M. Op de Beeck, N. Cong, H. Zhao, Y. Zhang, A. Menzel, I. A. Janssens (2015). Recent spring phenology shifts in western Central Europe based on multiscale observations. Global Ecology and Biogeography, 23, 1255-1263.

Gallo, K. P., L. Ji, B. Reed, J. Dwyer, J. Eidenshink (2004). Comparison of MODIS and AVHRR 16-day normalized difference vegetation index composite data. Geophysical Research Letters, 31, L07502, doi:10.1029/2003GL019385.

Gamon, J. A., K. F. Huemmrich, C. Y. S. Wong, I. Ensminger, S. Garrity, D. Y. Hollinger, A. Noormets, J. Peñuelas (2016). A remotely sensed pigment index reveals photosynthetic phenology in envergreen conifers. Proceedings of the National Academy of Sciences of the United States of America, 113, 13087-13092.

Gonsamo, A. and J. M. Chen (2016) Circumpolar vegetation dynamics product for global change study. Remote Sensing of Environment, 182, 13-26.

Güsewell, S. R. Furrer, R. Gehrig, B. Pietragalla (2017). Changes in temperature sensitivity of spring phenology with recent climate warming in Switzerland are related to shifts of the preseason. Global Change Biology, 23, 5189-5202.

Helman, D. (2018). Land surface phenology: what do we really 'see' from space? Science of The Total Environmenta, 618, 665-673.

Hird, J. N., G. J. McDermid (2009). Noise reduction of NDVI time series: An empirical comparison of selected techniques. Remote Sensing of Environment, 113, 248-258.

Jeong, S.-J., C.-H. Ho, H.-J. Gim, M. E. Brown (2011). Phenology shifts at start vs. end of growing season in temperate vegetation over the Northern Hemisphere for the period 1982-2008. Global Change Biology, 17, 2385-2399, doi: 10.1111/j.1365-2486.2011.02397.x

Jin, H., A. M. Jönsson, K. Bolmgren, O. Langvall, L. Eklundh (2017). Disentangling remotely-sensed plant phenology and snow seasonality at northern Europe using MODIS and the plant phenology index. Remote Sensing of Environment, 198, 203–212.

Kern, A., H. Marjanović, Z. Barcza. (2016). Evaluation of the quality of NDVI3g Dataset against collection 6 MODIS NDVI in central Europe between 2000 and 2013. Remote Sensing, 8, 955; doi:10.3390/rs8110955.

Linderholm, H. W. (2006). Growing season changes in the last century. Agricultural and Forest Meteorology, 137, 1-14.

Marshall, M., E. Okuto, Y. Kang, E. Opiyo, M. Ahmed. (2016). Global assessment of vegetation index and Phenology Lab (VIP) and Global Inventory Modeling and Mapping Studies (GIMMS) version 3 products. Biogeosciences, 13, 625-639.

Moulin, S., L. Kergoat, N. Viovy, G. Dedieu (1997). Global-scale assessment of vegetation phenology using NOAA/AVHRR satellite measurements. Journal of Climate, 10, 1154-1170.

Myneni, R. B., C. D. Keeling, C. J. Tucker, G. Asrar, R. R. Nemani (1997). Increased plant growth in the northern high latitudes from 1981 to 1991. Nature, 386, 698-702.

Oberbauer, S.F., S. C. Elmendorf, T. G. Troxler et al. (2013). Phenological response of tundra plants to background climate variation tested using the International Tundra Experiment. Philosophical Transactions of the Royal Society B: Biological Sciences, 368, 20120481. DOI: 10.1098/rstb.2012.0481

Park, T., S. Ganguly, H. Tømmervik, E. S. Euskirchen, K.-A. Høgda, S. R. Karlsen, V. Brovkin, R. R. Nemani, R. B. Myneni (2016). Changes in growing season duration and productivity of northern vegetation inferred from long-term remote sensing data. Environmental Research Letters, 11. 0.1088/1748-9326/11/8/084001

Peñuelas, J., I. Filella, X. Zhang, L. Llorens, R. Ogaya, F. Lloret, P. Comas, M. Estiarte, J. Terradas (2004). Complex spatiotemporal phonological shifts as a responses to rainfall changes. New Phytologist, 161, 837-846.

Piao, S., H. Nan, C. Huntingford, P. Ciais, P. Friedlingstein, S. Sitch, S. Peng, A. Ahlshtröm, J. G. Canadell, N. Cong, S. Levis, P. E. Levy, L. Liu, M. R. Lomas, J. Mao, R. B. Myneni, P. Peylin, B. Poulter, X. Shi, G. Yin, N. Viory, T. Wang, X. Wang, S. Zaehle, N. Zeng, Z. Zeng, A. Chen (2014). Evidence for a weakening relationship between interannual temperature variability and northern vegetation activity. Nature Communications, doi:10.1038/ncomms6018.

Pinzon, J. E., C. J. Tucker (2014). A non-stationary 1981-2012 AVHRR NDVI3g time series. Remote Sensing, 6, 6929-6960. doi:10.3390/rs6086929

Prevéy, J., M. Vellend, N. Rüger, R. D. Hollister, A. D. Bjorkman, I. H. Myers-Smith, S. C. Elmendorf, K. Clark, E. J. Cooper, B. Elberling, A. M. Fosaa, G. H. R. Henry, T. T. Høye, I. S. Jónsdóttir, K. Klanderud, E. Lévesque, M. Mauritz, U. Molau, S. M. Natali, S. F. Oberbauer, Z. A. Panchen, E. Post, S. B. Rumpf, N. M. Schmidt, E. A. G. Schuur, P. R. Semenchuk, T. Troxler, J. M. Welker, C. Rixen (2017). Greater temperature sensitivity of plant phenology at colder sites: implications for convergence across northern latitudes. Global Change Biology, 23, 2660-2671, DOI: 10.1111/gcb.13619.

Shen, M., Y. Tang, J. Chen, X. Zhu, Y. Zheng (2011). Influences of temperature and precipitation before the growing season on spring phenology in grasslands of the central and eastern Qinghai-Tibetan Plateau. Agricultural and Forest Meteorology, 151, 1711–1722. https://doi.org/10.1016/j.agrformet.2011.07.003

Shen M., Y. Tang Y, J. Chen, X. Yang, C. Wang, X. Cui, Y. Yang, L. Han, L. Li, J. Du, G. Zhang, N. C (2014). Earlier-Season Vegetation Has Greater Temperature Sensitivity of Spring Phenology in Northern Hemisphere. PLoS ONE 9(2): e88178. DOI:10.1371/journal.pone.0088178

Shen, M., N. Cong, R. Cao (2015). Temperature sensitivity as an explanation of the latitudinal pattern of green-up date trend in northern Hemisphere vegetation during 1982–2008. International Journal of Climatology, 35, 3707–3712. https://doi.org/10.1002/joc.422

Semenchuk, P. R., M. A. K. Gillespie, S. B. Rumpf, N. Baggesen, B. Elberling, E. J. Cooper (2016). High Arctic plant phenology is determined by snowmelt patterns but duration of phonological periods is fixed: an example of periodicity. Environmental Research Letters, 125006. DOI: 10.1088/1748-9326/11/12/125006.

Singh, R. K., T. Svystun, B. AlDahmash, A. M. Jönsson, R. P. Bhalerao (2017). Photoperiod- and temperature-mediated control of phenology in trees – a molecular perspective. New Phytologist, 213, 511-524.

Thompson, B.G. (2015). Using phase-spaces to characterize land surface phenology in a seasonally snow-covered landscape. Remote Sensing of Environment, 166, 178-190.

Tong, A. and Y. He (2013). Comparative analysis of SPOT, Landsat, MODIS and AVHRR normalized difference vegetation index data on the estimation of leaf area index in a mixed grassland ecosystem. Journal of Applied Remote Sensing, 7, 073599-1-15.

Wang, S., B. Yang, Q. Yang, L. Lu, X. Wang, Y. Peng (2016). Temporal trends and spatial variability of vegetation phenology over the Northern Hemisphere during 1982-2012. PLoS ONE, 11, e0157134. doi:10.1371/journal.pone.0157134

Wu, X., H. Liu, X. Li, S. Piao, P. Ciais, W. Guo, Y. Yin, B. Poulter, C. Peng, N. Viory, N. Vuichard, P. Wang, Y. Huang (2017). Higher temperature variability reduces temperature sensisitivity of vegetation growth in Northern Hemisphere. Geophysical Research Letters, Doi: 10.1002/2017GL073285

Xu, X., W.J. Riley, C. D. Koven, G. Jia (2018). Observed and simulated sensitivities of spring greenup to preseason climate in northern temperate and boreal regions. Journal of Geophysical Research: Biogeoscience, 123: 60-78. doi: 10.1002/2017jg004117

Way, D. A. and R. A. Montgomery (2015). Photoperiod constraints on tree phenology, performance and migration in a warming world. Pland, Cell and Environment, 38, 1725-1736.

Yang, B., M. He, V. Shishov, I. Tychkov, E. Vaganov, S. Rossi, F. C. Ljungqvist, A. Bräuning, J. Grieβinger (2017). New perspective on spring vegetation phenology and global climate change based on Tibetan Plateau tree-ring data.

Proceedings of the National Academy of Sciences of the United States of America, 114, 6966-6971.

Yu, H., E. Luedeling, J. Xu (2010). Winter and spring warming result in delayed spring phenology on the Tibetan Plateau. Proceedings of the National Academy of Sciences of the United States of America, 107, 22151-22156.

Zeng, H., G. Jia, B. C. Forbes (2013a). Shifts in Arctic phenology in response to climate and anthropogenic factors as detected from multiple satellite time series. Environmental Research Letters, 8, 035036. Doi:10.1088/1748-9326/8/3/035036.

Zeng, H. and G. Jia (2013). Impacts of snow cover on vegetation phenology in the Arctic from satellite data. Advances in Atmospheric Sciences, 30, 1421-1432.

Zhang, X., Friedl, M.A., Schaaf, C.B., Strahler, A.H., Hodges, J.C.F., Gao, F., Reed, B.C., Huete, A. (2003). Monitoring vegetation phenology using MODIS. Remote Sensing of Environment, 84, 471–475.

Zhang, G., Y. Zhang, J. Dong, X. Xiao (2013). Green-up dates in the Tibetan Plateau have continuously advanced from 1982-2011. Proceedings of the National Academy of Sciences of the United States of America, 110, 4309-4314.

Zhang, X., L. Liu, D. Yan (2017). Comparisons of global land surface seasonality and phenology derived from AVHRR, MODIS, and VIIRS data. Journal of Geophysical Research: Biogeosciences, 122, 1506-1525.

Zhou, J., L. Jia, M. Menenti (2015). Reconstruction of global MODIS NDVI time series: Performance of Harmonic ANalysis of Time Series (HANTS). Remote Sensing of Environment, 163, 217-228. DOI: 10.1016/j.rse.2015.03.018

Figure Captions:

Figure 1 (a) Correlation between MODIS and GIMMS inferred inter-annual D_{SG} over 2001-2013 ($p < 0.1$), (b) the difference between GIMMS and MODIS inferred $\overline{D}_{SG}$ (days, $D_{SG}^{M} - D_{SG}^{G}$), and (c) GIMMS , (d) MODIS inferred trend of spring greenup date (D_{SG}) over 2001-2013(days yr^{-1}).

Figure 2 Anomalies of spring greenup date for mid-latitude (30-50ºN, a, c, e) and high latitude (>50ºN, b, d, f) in relative to mean D_{SG} over 2001-2013 for GIMMS and MODIS.

Figure 3 Pearson correlation coefficient (PCC) between preseason temperature (T_m) and date of spring greenup (D_{SG}) for GIMMS (a) and MODIS(b) and Pearson correlation coefficient (PCC) between preseason precipitation (P_t) and date of spring greenup (D_{SG}) for GIMMS (c) and MODIS(d).

Figure 4 Spring greenup sensitivity to preseason temperature (days °C^{-1}) for GIMMS (a) and MODIS (b) and spring greenup sensitivity to preseason precipitation (days $\%^{-1}$ of precipitation increases) for GIMMS (c) and MODIS (d).

Figure 5 The comparison of inter-biome SG sensitivity to preseason temperature for IGBP land cover types for GIMMS over 1982-2005 and 2001-2013 and MODIS over 2001-2013. We used the IGBP land cover classification for 9 biomes in 2012: Evergreen Needleleaf Forest (ENF), Deciduous Needleleaf Forest (DNF), Deciduous Broadleaf forest (DBF), Mixed Forest (MF), Open Shrublands (OS), Woody Savannas (WS), Grassland (GL), Permanent Wetland (PW), and Cropland (CP). We distinguish the Arctic grassland to the north of 60°N (GLN), from temperate grassland in the south (GLS) due to their expected differences in climate and controls on phenology.

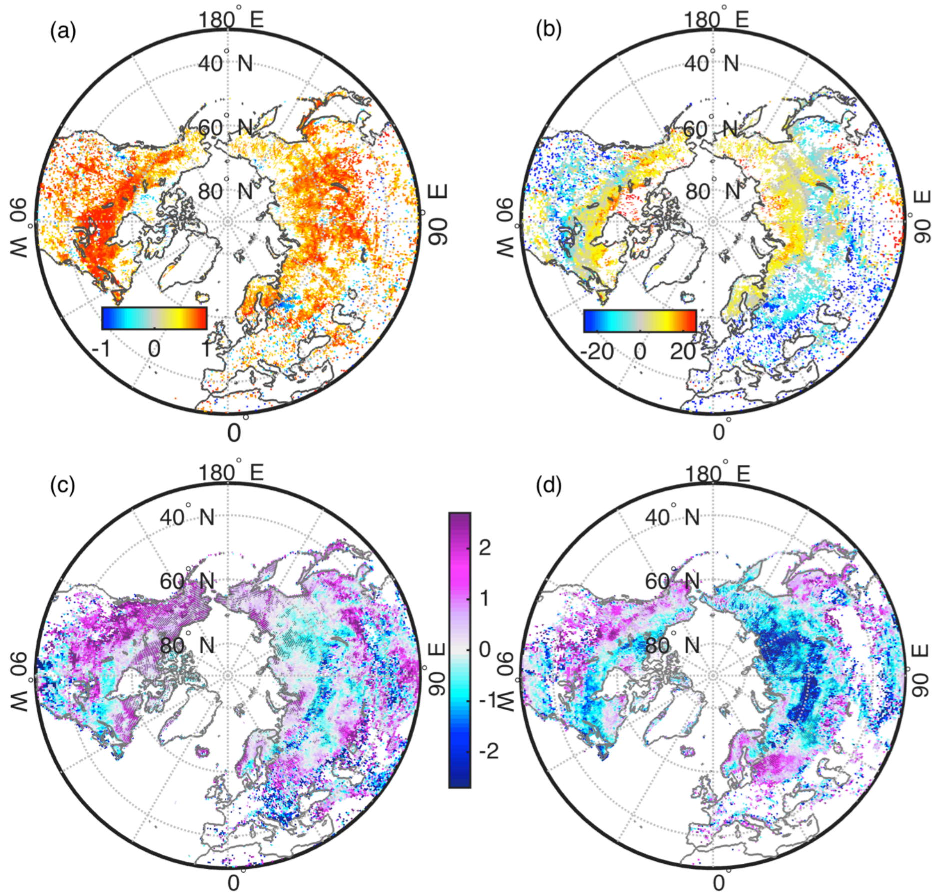

Figure 1 (a) Correlation between MODIS and GIMMS inferred inter-annual D_{SG} over 2001-2013 (p < 0.1), (b) the difference between GIMMS and MODIS inferred $\overline{D}_{SG}$ (days, $D_{SG}^{M} - D_{SG}^{G}$), and (c) GIMMS , (d) MODIS inferred trend of spring greenup date (D_{SG}) over 2001-2013(days yr^{-1}).

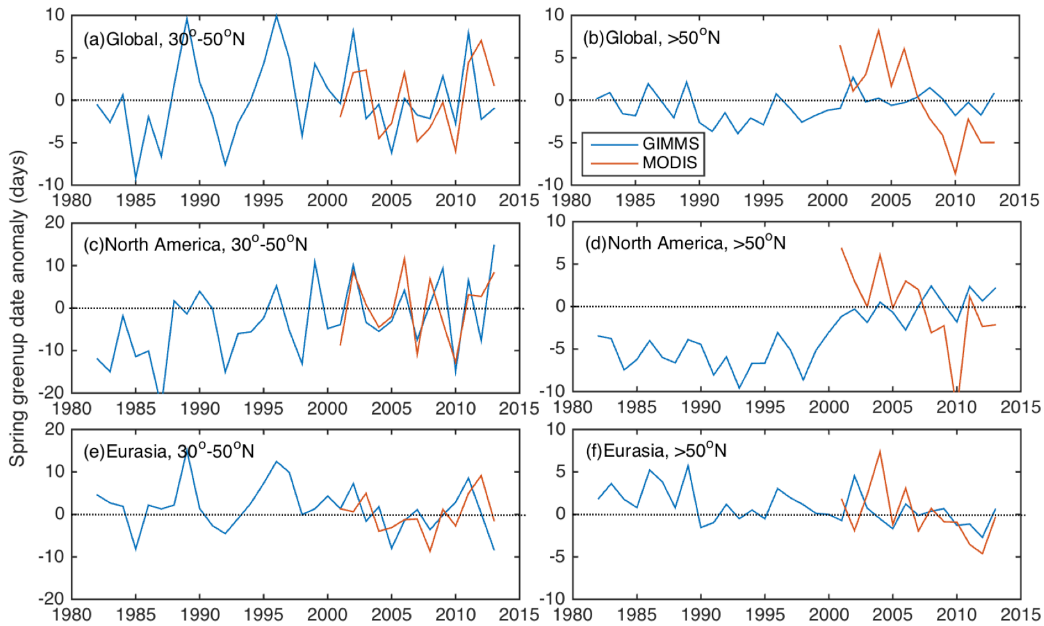

Figure 2 Anomalies of spring greenup date for mid-latitude (30-50° N, a, c, e) and high latitude (>50° N, b, d, f) in relative to mean D_{SG} over 2001-2013 for GIMMS and MODIS.

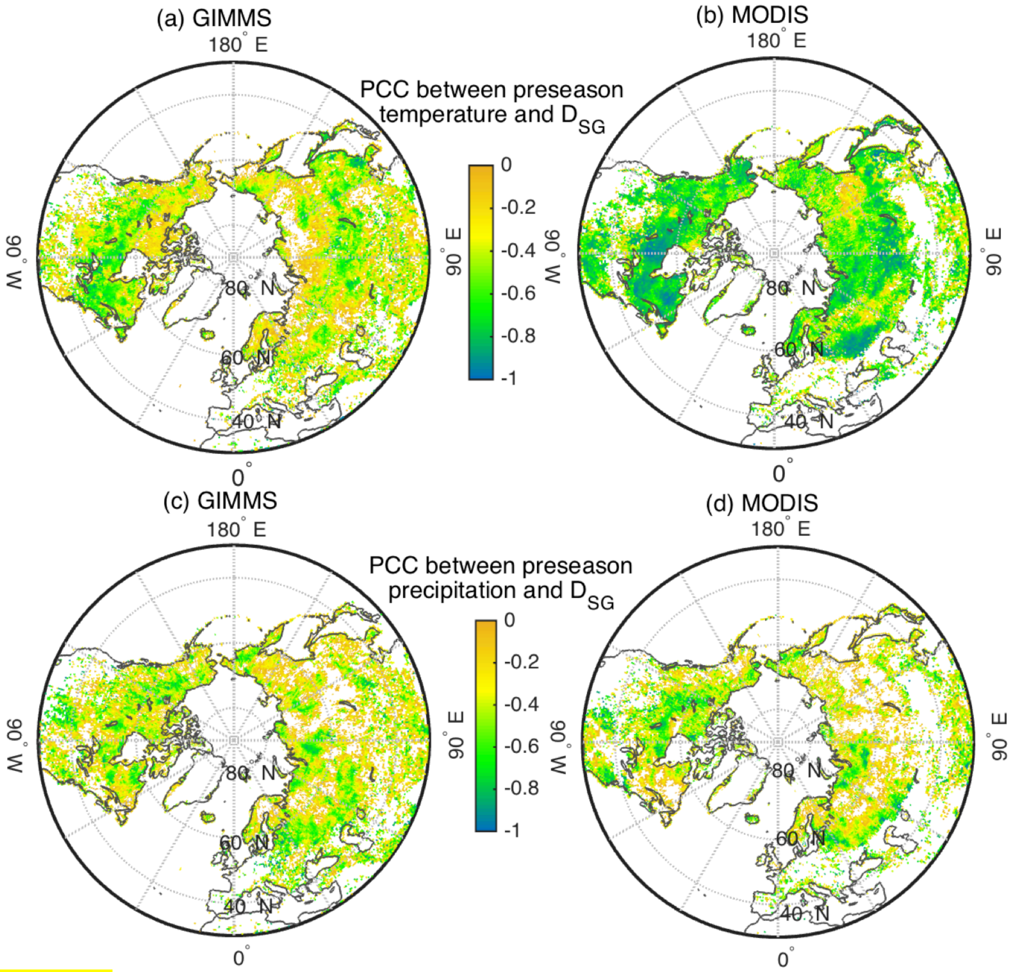

Figure 3 Pearson correlation coefficient (PCC) between preseason temperature (T_m) and date of spring greenup (D_{SG}) for GIMMS (a) and MODIS(b) and Pearson correlation coefficient (PCC) between preseason precipitation (P_t) and date of spring greenup (D_{SG}) for GIMMS (c) and MODIS(d).

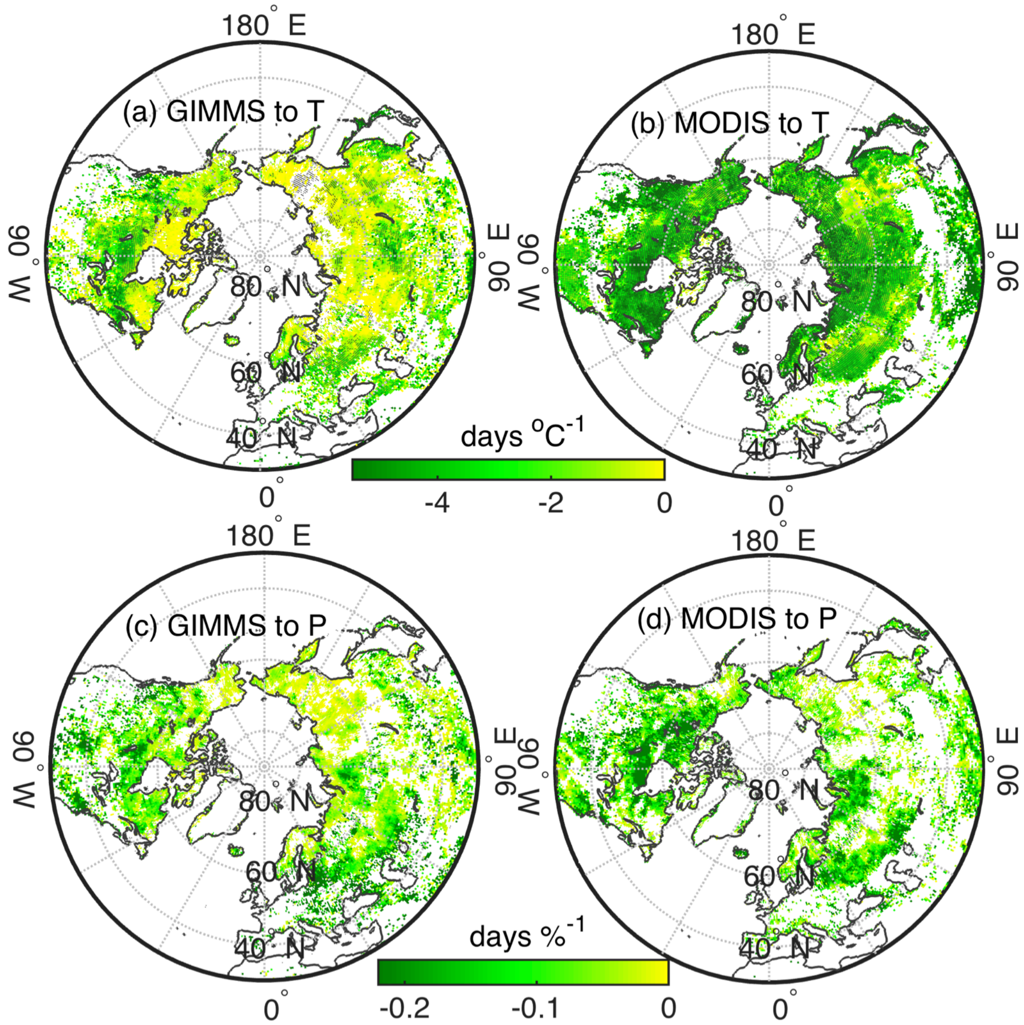

Figure 4 Spring greenup sensitivity to preseason temperature (days °C^{-1}) for GIMMS (a) and MODIS (b) and spring greenup sensitivity to preseason precipitation (days %$^{-1}$ of precipitation increases) for GIMMS (c) and MODIS (d).

.

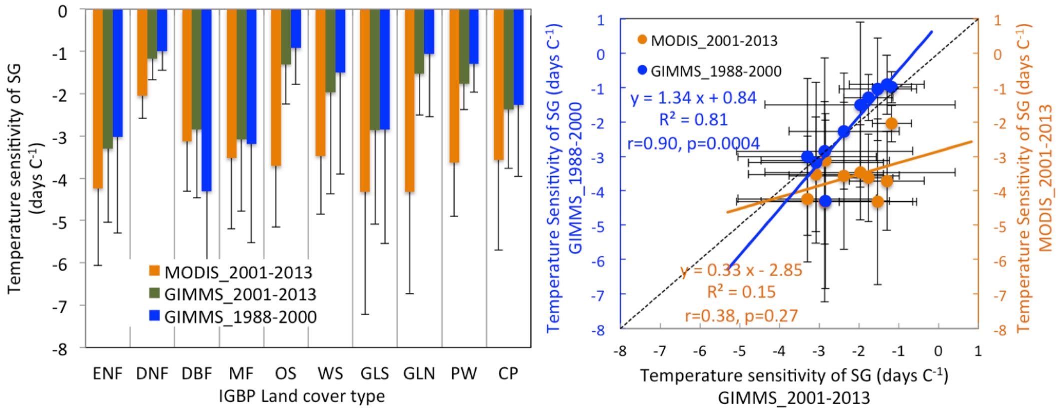

Figure 5 The comparison of inter-biome SG sensitivity to preseason temperature for IGBP land cover types for GIMMS over 1982-2005 and 2001-2013 and MODIS over 2001-2013. We used the IGBP land cover classification for 9 biomes in 2012: Evergreen Needleleaf Forest (ENF), Deciduous Needleleaf Forest (DNF), Deciduous Broadleaf forest (DBF), Mixed Forest (MF), Open Shrublands (OS), Woody Savannas (WS), Grassland (GL), Permanent Wetland (PW), and Cropland (CP). We distinguish the Arctic grassland to the north of 60°N (GLN), from temperate grassland in the south (GLS) due to their expected differences in climate and controls on phenology.

Supplement Information for

Spring phenology inferred from two remotely sensed vegetation indices time series: confidence and uncertainty

Xiyan Xu[1, 2], William J. Riley[2], Charles D. Koven[2], Gensuo Jia[1*]

[1]Key Laboratory of Regional Climate-Environment for Temperate East Asia, Institute of Atmospheric Physics, Chinese Academy of Sciences, Beijing 100029, China

[2]Climate and Ecosystem Sciences Division, Lawrence Berkeley National Laboratory, Berkeley, California, USA

Corresponding Author:

Dr. Gensuo Jia

Key Laboratory of Regional Climate-Environment for Temperate East Asia,

Institute of Atmospheric Physics, Chinese Academy of Sciences,

Beijing 100029, China

Email address: jiong@tea.ac.cn

Phone number: +86-10-82995314

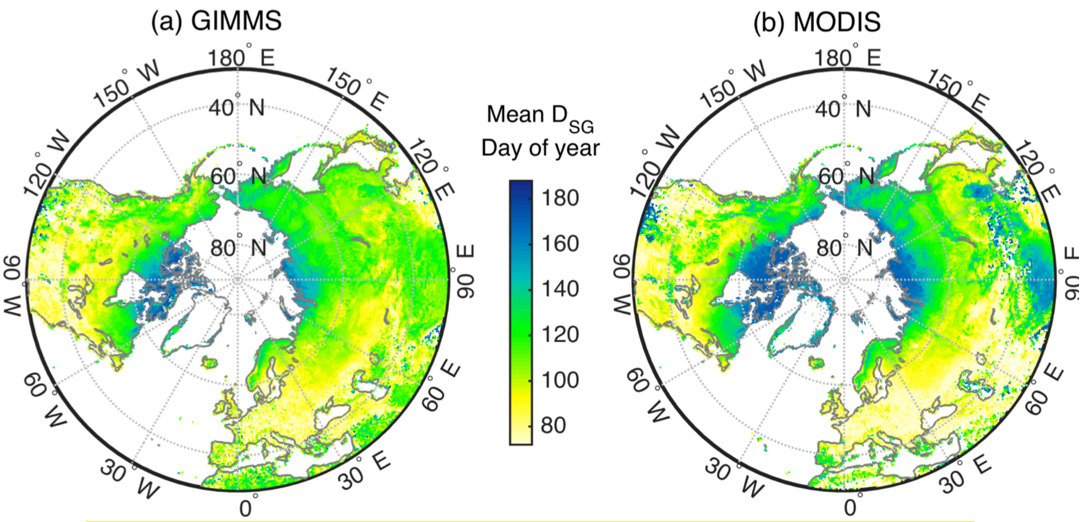

Figure S1 GIMMS (a) and MODIS (b) inferred mean D_{SG} over 2001-2013

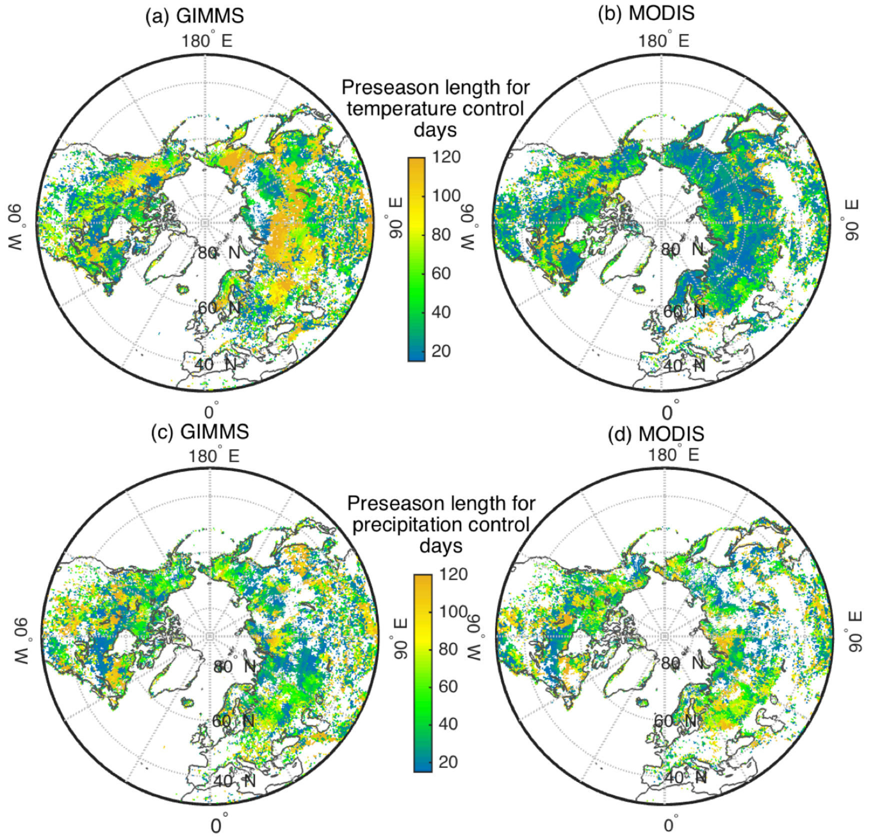

Figure S2 Mean preseason length of temperature control corresponding to GIMMS spring greenup ($\overline{L}_{PT}^{G}$, days) and MODIS spring greenup ($\overline{L}_{PT}^{M}$, days) and mean preseason length of precipitation control corresponding to GIMMS spring greenup ($\overline{L}_{PP}^{G}$, days) and MODIS greenup ($\overline{L}_{PP}^{M}$, days).

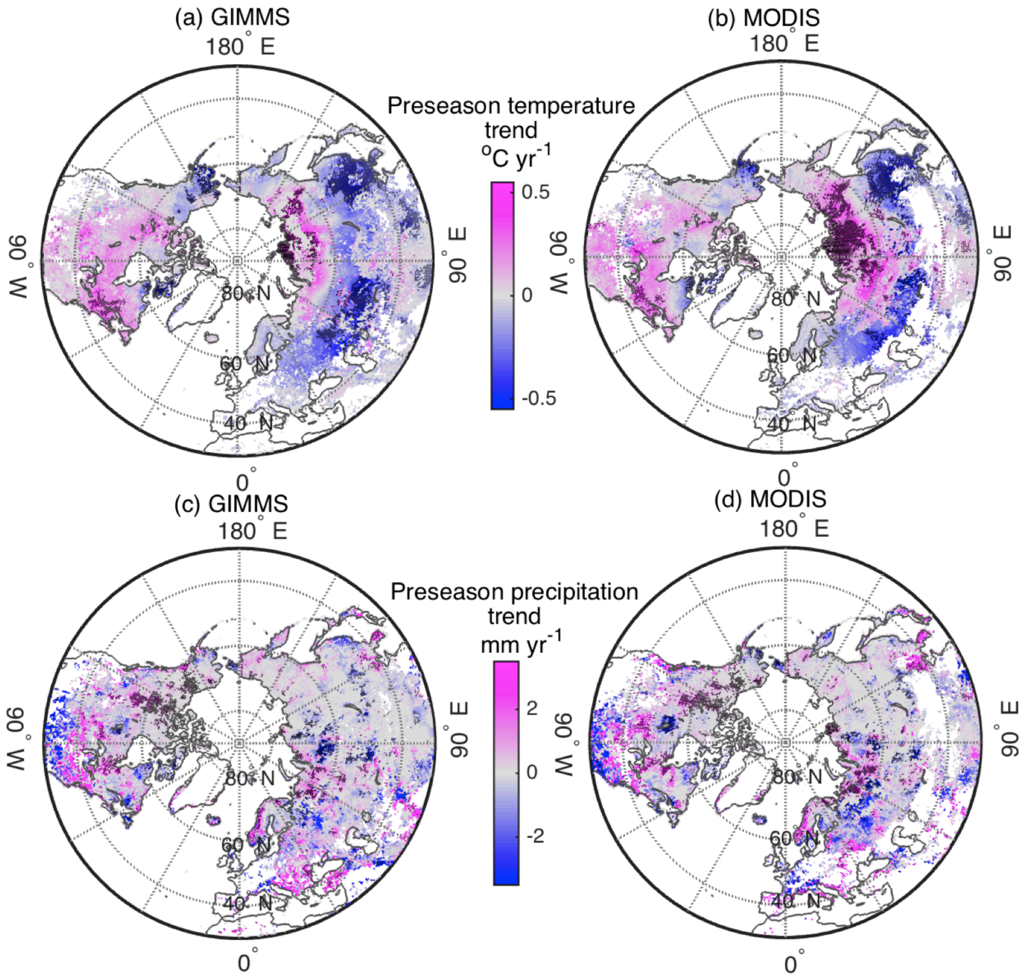

Figure S3 The preseason temperature trend (°C yr^{-1}) calculated from CRUNCEP correlated to spring greenup date inferred from GIMMS (a) and MODIS (b) NDVI and precipitation trend (mm yr^{-1}) calculated from CRUNCEP correlated to spring greenup date inferred from GIMMS (c) and MODIS (d) NDVI. The shaded regions indicate that the trend is significant ($p < 0.1$).

Table S1 The spring greenup shift (days per decade) as inferred from Normalized Difference Vegetation Index (NDVI) from satellite data

NDVI Data	Period	Region	Shift (days decade^{-1})	Reference
PAL	1981-1991	>=40N	-8	Myneni et al., 1997
GIMMS	1981-1999	Eurasia	-3.3	Zhou et al., 2001
GIMMS	1981-1999	N. America	-4.4	Zhou et al., 2001
AVHRR	1982-1991	45-75	-6.2	Tucker et al., 2001
AVHRR	1992-1999	45-75	-2.4	Tucker et al., 2001
AVHRR	1982-1990	Inner Mongolia	0	Lee et al., 2002
PAL	1982-2001	Europe	-5.4	Stockli and Vidale, 2004
PAL	1985-1999	N. America	-6.6	de Beurs and Henebry, 2005
PAL	1985-2000	Eurasia	-4.5	de Beurs and Henebry, 2005
GIMMS	1982-1999	Temperate China	-7.9	Piao et al., 2006
PAL	1982-1999	East Asia	-7	Jeong et al., 2009
GIMMS	1982-2003	Global	-3.8	Julien & Sobrino, 2009
GIMMS	1982-2006	Fennoscandia	-2.7	Karlsen et al., 2009
GIMMS	1982-1999	N. Hemisphere	-2.9	Jeong et al., 2011
GIMMS	2002-2008	N. Hemisphere	-0.3	Jeong et al., 2011
MODIS	2000-2010	>60N, Arctic	-4.7	Zeng et al., 2011
MODIS	2000-2010	>60N, N. America	-11.5	Zeng et al., 2011
MODIS	2000-2010	>60N, Eurasia	-2.7	Zeng et al., 2011
GIMMS	1982-2008	>60N, Arctic	-0.5	Zeng et al., 2011
GIMMS	1982-2008	>60N, N. America	-0.8	Zeng et al., 2011
GIMMS	1982-2008	>60N, Eurasia	-0.3	Zeng et al., 2011
GIMMS SPOT-VGT	1982-2011	Tibetan Plateau	-10.4	Zhang et al., 2013
GIMMS	1982-2011	Fennoscandia	-11.8	Høgda et al., 2013
MODIS	2001-2012	U.S.	-4.8	Keenan et al., 2014
MODIS	2002-2014	Inner Mongolia	-4.5	Gong et al., 2015
GIMMS	1982-2011	U.S. Great Basin	-0.1	Tang et al., 2015
GIMMS	1982-2002	N. Hemisphere	-1.9	Wang et al., 2016
MODIS	2002-2012	N. Hemisphere	-5.9	Wang et al., 2016
GIMMS	1982-2012	Tibetan Plateau	0	Ding et al., 2016

MODIS: Moderate Resolution Imaging Spectroradiometer
AVHRR: Advanced Very High Resolution Radiometer
GIMMS: Global Inventory Modeling and Mapping Studies
PAL: Pathfinder AVHRR Land
GAC: Global area cover

Table S2. The number of pixels for the calculation of D_{SG} sensitivity to preseason temperature ($p<0.1$) for each biome

Veg. Type*	1988-2000	2001-2013	
	GIMMS	GIMMS	MODIS
ENF	1477	556	1677
DNF	356	202	339
DBF	119	26	96
MF	2700	966	2860
OS	4691	616	5371
WS	1204	168	1397
GLS	2076	630	1273
GLN	874	143	545
PW	327	95	330
CP	1019	587	791

*We used the IGBP land cover classification for 9 biomes in 2012: Evergreen Needleleaf Forest (ENF), Deciduous Needleleaf Forest (DNF), Deciduous Broadleaf forest (DBF), Mixed Forest (MF), Open Shrublands (OS), Woody Savannas (WS), Grassland (GL), Permanent Wetland (PW), and Cropland (CP). We distinguish the Arctic grassland to the north of 60°N (GLN), from temperate grassland in the south (GLS) due to their expected differences in climate and controls on phenology.

Reference

De Beurs, K. M. and G. M. Henebry (2005) Land surface phenology and temperature variation in the international geosphere-biosphere program high-latitude transects. Global Change Biology, 11, 779-790. Doi: 10.1111/j.1365-2486.2005.00949.x

Ding, M., L. Li, Y. Nie, Q. Chen, Y. Zhang (2016) Spatio-temporal variation of spring phenology in Tibetan Plateau and its linkage to climate change from 1982 to 2012. Journal of Mountain Science, 13, 83-94.

Gong, Z., K. Kawamura, N. Ishikawa, M. Goto, T. Wulan, D. Alateng, T. Yin, Y. Ito (2015) MODIS normalized difference vegetation index (NDVI) and vegetation phenology dynamics in the Inner Mongolia grassland. Solid Earth, 6, 1185-1194. Doi: 10.5194/se-6-1185-2015

Høgda, K. A., H. Tømmervik, S. R. Karlsen (2013) Trends in the start of the growing season in Fennoscandia 1982-2011. Remote Sensing, 5, 4304-4318. Doi: 10.3390/rs5094304

Jeong, S.J., *C.* H. Ho*,* J. H. Jeong *(*2009*)* Increase in vegetation greenness and decrease in spring time warming over East Asia*.* Geophysical Research Letters*,* 36*,* L0270*, doi: DOI:* 10.1029/2008GL036583*.*

Jeong, S.-J., C.-H. Ho, H.-J. Gim, M. E. Brown (2011) Phenology shifts at start vs. end of growing season in temperate vegetation over the Northern Hemisphere for the period 1982-2008. Global Change Biology, 17, 2385-2399, doi: 10.1111/j.1365-2486.2011.02397.x

Julien, Y., J. A. Sobrino *(*2009*)* Global land surface phenology trends from GIMMS database*.* International Journal of Remote Sensing*,* 30*,* 3495–3513*.*

Karlsen, S.R., K. A. Høgda, F. E. Wielgolaski, A. Tolvanen, H. Tommervik, J. Poikolainen, E. Kubin (2009) Growing-season trends in Fennoscandia 1982–2006, determined from satellite and phenology data. Climate Research, 39, 275–286.

Keenan, T. F., B. Darby, E. Felts, O. Sonnentag, M. A. Friedl, K. Hufkens, J. O’Keefe, S. Klosterman, J. W. Munger, M. Toomey, A. D. Richardson (2014) Tracking forest phenology and seasonal physiology using digital repeat photography: a critical assessment. Ecological Applications, 24, 1478-1489. Doi:10.1890/13-0652.1

Lee, R., F. Yu, K. P. Price, J. Ellis, P. Shi (2002) Evaluating vegetation phonological patterns in Inner Mongolia using NDVI time-series analysis. International Journal of Remote Sensing, 23, 2505-2512. Doi:10.1080/01431160110106087

Myneni, R. B., C. D. Keeling, C. J. Tucker, G. Asrar, R. R. Nemani (1997) Increased plant growth in the northern high latitudes from 1981 to 1991, Nature, 386, 698-702.

Piao, S. L., J. Y. Fang, L. M. Zhou, P. Ciais, B. Zhu(2006) Variations in satellite-derived phenology in China’s temperate vegetation. Global Change Biology, 12, 672-685.

Stöckli, R. and P. L. Vidale (2004) European plant phenology and climate as seen in a 20-year AVHRR land-surface parameter dataset. International Journal of Remote Sensing, 25, 3303-3330. Doi: 10.1080/01431160310001618149

Tang, G., J. A. Arnone III, P. S. J. Verburg, R. L. Jasoni, L. Sun (2015) Trends and climatic sensitivities of vegetation phenology in semiarid and arid ecosystems in the US Great Basin during 1982-2011. Biogeosciences, 12, 6985-6997. Doi:10.5194/bg-12-6985-2015

Tucker, C. J., D. A. Slayback, J. E. Pinzon, S. O. Los, R. B. Myneni, M. G. Taylor (2001) Higher northern latitude NDVI and growing season trends from 1982 to 1999. International Journal of Biometeorology, 45, 184-190. Doi: 10.1007/s00484-001-0109-9.

Wang, S., B. Yang, Q. Yang, L. Lu, X. Wang, Y. Peng (2016) Temporal trends and spatial variability of vegetation phenology over the Northern Hemisphere during 1982-2012. PLoS ONE, 11, e0157134. doi:10.1371/journal.pone.0157134

Zeng, H., G. Jia, H. Epstein (2011) Recent Changes in Phenology over the northern high latitudes detected from multi-satellite data. Environmental Research Letters, 045508. Doi: 10.1088/1748-9326/6/045508

Zhang, G., Y. Zhang, J. Dong, X. Xiao (2013) Green-up dates in the Tibetan Plateau have continuously advanced from 1982-2011, Proceedings of the National Academy of Sciences of the United States of America, 110, 4309-4314.

Zhou, L., C. J. Tucker, R. K. Kaufmann, D. Slayback, N. V. Shabanov, R. B. Myneni (2001) Variations in northern vegetation activity inferred from satellite data of vegetation index during 1981-1999. Journal of Geophysical Research: Atmosphere, 106, 20069-20083. Doi: 10.1029/2000JD000115